

This article was downloaded by:

On: 14 January 2011

Access details: *Access Details: Free Access*

Publisher *Taylor & Francis*

Informa Ltd Registered in England and Wales Registered Number: 1072954 Registered office: Mortimer House, 37-41 Mortimer Street, London W1T 3JH, UK



Molecular Simulation

Publication details, including instructions for authors and subscription information:

<http://www.informaworld.com/smpp/title~content=t713644482>

The activity coefficient of high density systems with hard-sphere interactions: the application of the IGCMC method

S. Lamperski^a; M. Płuciennik^a

^a Department of Physical Chemistry, Faculty of Chemistry, A. Mickiewicz University, Poznań, Poland

First published on: 10 September 2009

To cite this Article Lamperski, S. and Płuciennik, M.(2010) 'The activity coefficient of high density systems with hard-sphere interactions: the application of the IGCMC method', *Molecular Simulation*, 36: 2, 111 — 117, First published on: 10 September 2009 (iFirst)

To link to this Article: DOI: 10.1080/08927020903124577

URL: <http://dx.doi.org/10.1080/08927020903124577>

PLEASE SCROLL DOWN FOR ARTICLE

Full terms and conditions of use: <http://www.informaworld.com/terms-and-conditions-of-access.pdf>

This article may be used for research, teaching and private study purposes. Any substantial or systematic reproduction, re-distribution, re-selling, loan or sub-licensing, systematic supply or distribution in any form to anyone is expressly forbidden.

The publisher does not give any warranty express or implied or make any representation that the contents will be complete or accurate or up to date. The accuracy of any instructions, formulae and drug doses should be independently verified with primary sources. The publisher shall not be liable for any loss, actions, claims, proceedings, demand or costs or damages whatsoever or howsoever caused arising directly or indirectly in connection with or arising out of the use of this material.

The activity coefficient of high density systems with hard-sphere interactions: the application of the IGCMC method

S. Lamperski* and M. Płuciennik

Department of Physical Chemistry, Faculty of Chemistry, A. Mickiewicz University, Grunwaldzka 6, 60-780 Poznań, Poland

(Received 27 March 2009; final version received 15 June 2009)

The inverse grand-canonical Monte Carlo (IGCMC) technique is used to calculate the activity coefficients of the following hard-sphere systems: one-component fluid, binary mixture and solvent primitive model (SPM) electrolyte. The calculations for a one-component fluid are performed at different densities. The components of a binary mixture differ in diameters (300 and 500 pm) with the results being presented for different density and composition of a mixture. For the SPM model, simulations are performed for a 1:1 electrolyte at different electrolyte concentrations at the packing fraction equal to 0.3. Ions and solvent molecules of the same or different sizes are considered. The results are compared with those reported by Adams (one-component fluid), with those calculated using the Ebeling and Scherwinski equation (one-component fluid and binary mixture) and with the predictions from the symmetric Poisson–Boltzmann theory and the mean spherical approximation (SPM electrolyte).

Keywords: activity coefficient; inverse grand-canonical Monte Carlo method; hard-sphere interactions; solvent primitive model electrolyte; GCMC simulation

1. Introduction

The chemical potential is perhaps the most important function describing the thermodynamic properties of a fluid. Its essential component, the activity coefficient, describes all the deviations from ideality. The activity coefficient can be determined experimentally, calculated from the statistical thermodynamics or obtained from the numerical molecular simulations. Unfortunately, the entropy-related functions like the free energy or the chemical potential cannot be estimated directly from the Monte Carlo (MC) simulation in the canonical ensemble [1] as this method samples the regions making small contributions to the configuration partition function. However, application of the Gibbs–Helmholtz equation [1] allows us to calculate the free energy from MC simulations, but the method requires many simulations at different temperatures. Widom [2] proposed a simpler and more attractive technique. It consists of inserting a particle into the simulation box, which tests the intermolecular interactions. The individual ionic activity coefficients can be calculated by this method [3,4], but the extrapolation of the results to the thermodynamic limit is required as the results depend on the number of particles in the simulation box. Another method used to calculate the activity coefficient is the MC simulation in the grand-canonical ensemble (GCMC). This technique was applied by Adams [5] among others to calculate the chemical potential of hard-sphere fluids and by Valleau and Cohen

[6,7] to evaluate the mean activity coefficient of electrolyte. A drawback of the GCMC method is that it can often be inconvenient to use as it gives the concentration of particles for a specified activity coefficient. Recently, the GCMC method has been modified by Lamperski [8], and in the modified form it allows evaluation of the activity coefficient for a specified concentration of particles. It is called the inverse GCMC method (IGCMC) as it uses the GCMC techniques, but it works in the reverse direction. Malasics et al. [9] have proposed two other efficient iterative MC algorithms in the GC ensemble to determine the chemical potentials. These authors applied their method to the Lennard-Jones fluids and to the primitive electrolyte mixture.

The IGCMC technique was successfully used to calculate the individual and mean activity coefficients of the 1:1, 2:2, 2:1 and 3:1 PM electrolyte with ions of the same and different size at different electrolyte concentrations [8]. The results for ions of the same size were compared with the corresponding data obtained by Valleau and Cohen [6], while the results for a 1:1 electrolyte with ions of different size were compared with those of Sloth and Sørensen [4], and with the theoretical predictions of Sloth and Sørensen [10], Molero et al. [11] and Outhwaite et al. [12,13]. The results obtained by the IGCMC method were comparable with those obtained or predicted by other methods. The advantage of IGCMC over GCMC is that the former can be used to compute also

*Corresponding author. Email: slamper@amu.edu.pl

the individual ionic activity coefficients which cannot be done by the standard GCMC method.

In this paper, we want to demonstrate that the IGCMC method gives correct results for hard-sphere fluids at high densities. The following three systems are the objects of our investigation here: (1) one-component fluid, (2) binary mixture and (3) solvent primitive model (SPM) electrolyte.

2. The model

The simplest model that takes into account the finite size of the molecules is the hard-sphere model. Representing the molecules of the i th kind by hard spheres of the diameter d_i , the pair potential of interaction is given by

$$u^{\text{hs}}(r_{ij}) = \begin{cases} 0, & r_{ij} > d_{ij} \\ \infty, & r_{ij} \leq d_{ij} \end{cases}, \quad (1)$$

where r_{ij} is the distance between the centres of two interacting molecules (hard spheres) and d_{ij} is given by

$$d_{ij} = \frac{d_i + d_j}{2}. \quad (2)$$

The SPM electrolyte model is a simple yet non-trivial model of an electrolyte that takes into account the molecular nature of solvent. We assume that the ions and solvent molecules are represented by hard spheres of diameter d_{\pm} and d_s , respectively. The ions have additionally a point electric charge $z_i e$ embedded at the centre (e is the elementary charge and z_i is the charge number of ions of the i th kind). The inter-ionic electrostatic interactions are described by

$$u^e(r_{ij}) = \frac{z_i z_j e^2}{4\pi\epsilon_0\epsilon_r r_{ij}}, \quad (3)$$

where ϵ_r is the relative permittivity of the solvent and ϵ_0 is the vacuum permittivity. The importance of the SPM and hard-sphere models stems from the fact that they can be used both in molecular MC simulations and theoretical studies. Consideration of solvent molecules makes the model of electrolyte more realistic and allows investigation at densities similar to those of the real systems.

3. The method

In the GC ensemble, the volume, V , temperature, T , and the chemical potential, μ , are constant, while the number of molecules, N , and the energy, E , fluctuate. In the GCMC technique, the activity coefficient is used to calculate the concentration of particles. Recently, Lamperski [8] has shown that this method can be made to work in the reverse direction. The new

technique, called the IGCMC, can be used to estimate the activity coefficient of particles for their specified concentration. We will describe the performance of this method with an example of a one-component fluid. Extension to a multi-component solution is straightforward and gives the individual activity coefficients. The technique consists of m short GCMC simulations in each of which n number of configurations are generated. As in the GCMC technique, we input the activity coefficient ($\ln \gamma_l$) into each l th sub-simulation and obtain the average number $\langle N \rangle_l$ of molecules. This number is compared with the number N^0 which corresponds to the specified concentration c

$$N^0 = 1000cN_A V, \quad (4)$$

where N_A is the Avogadro constant and V is the volume of the simulation box. If $\langle N \rangle_l$ is lower than N^0 , then the value of $\ln \gamma_l$ is increased by a small amount, e.g. 0.2%, otherwise it is decreased by 0.2%. When the simulation is finished, the average value of the activity coefficients evaluated after each sub-simulation is calculated to give the final activity coefficient

$$\ln \gamma = \frac{1}{m} \sum_{l=1}^m \ln \gamma_l. \quad (5)$$

The simulations were carried out for $n = 20,000$ configurations and $m = 7500$ sub-simulations. The first 2500 sub-simulations were used to equilibrate the system.

In the IGCMC, as in GCMC, there are three equally probable moves: displacement, insertion and removal. In the first move, a particle selected at random is displaced to a new random position in the simulation box. The acceptance of displacement is given by

$$\text{acc}(m \rightarrow n) = \min\{1, \exp[-(u_n - u_m)/kT]\}, \quad (6)$$

where u_m is the potential energy of the configuration before displacement, u_n is the potential energy of the new trial configuration and k is the Boltzmann constant.

In the second move, a molecule is inserted at a random position in the simulation box. The acceptance of insertion is described by the equation

$$\text{acc}(N \rightarrow N+1) = \min\left[1, \exp\left(-\Delta u_i/kT + \ln \frac{\gamma N^0}{N+1}\right)\right], \quad (7)$$

where Δu_i is the potential of insertion and N is the current number of molecules.

In the last move, a particle selected at random is removed from the box. The acceptance of this move is

$$\text{acc}(N \rightarrow N - 1) = \min \left[1, \exp \left(-\Delta u_r / kT + \ln \frac{N}{\gamma N^0} \right) \right], \quad (8)$$

where Δu_r is the potential of removal.

4. Results and discussion

4.1 Hard-sphere one-component system

First, we consider a one-component hard-sphere fluid. The IGCMC technique was applied to calculate the activity coefficient. The simulations were performed for the following reduced densities ρ^* : 0.1, 0.2, 0.3, 0.4, 0.5, 0.6, 0.7, 0.8 at the diameter $d = 400$ pm ($\rho^* = \rho d^3$, ρ is the number density, $\rho = N^0/V = 1000cN_A$). The results are shown in Figure 1 and collected in Table 1 where they are compared with the corresponding Adams [5] data and the theoretical predictions obtained from the Ebeling and Scherwinski equation [14]. The value of the activity coefficient increases with increasing density of a system. Our results and those obtained by Adams are nearly identical, while the predictions evaluated from the Ebeling and Scherwinski's equation are also very similar, but systematically lower. For a comparison with the results of Adams, our results in column 1 of Table 1 are presented in terms of the reduced density ρ^* . The corresponding packing fractions η ($= \pi \rho^*/6$) are given in column 2 and are used in Figure 1.

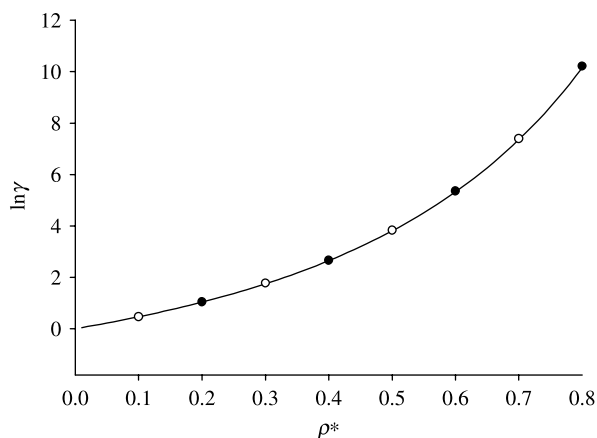


Figure 1. The activity coefficient of one-component hard-sphere fluid (solid circles, simulation; open circles, Adams' results [5]; solid lines, the Ebeling and Scherwinski equation).

Table 1. Activity coefficients of one-component hard-sphere fluid.

ρ^*	η	$\ln \gamma$		
		IGCMC	Adams [5]	Ebeling and Scherwinski equation [14]
0.1	0.0524	0.465	0.466	0.464
0.2	0.1047	1.040	1.043	1.035
0.3	0.1571	1.764	1.770	1.747
0.4	0.2094	2.656	2.651	2.648
0.5	0.2618	3.830	3.832	3.807
0.6	0.3142	5.357	5.359	5.326
0.7	0.3665	7.392	7.391	7.359
0.8	0.4189	10.211	10.210	10.153

4.2 Binary mixture of hard spheres

The second model studied was a two-component mixture of hard spheres of different diameters, d_1 (300 pm) and d_2 (500 pm). The simulations were carried out for the following packing fractions, η : 0.05, 0.10, 0.15, 0.20, 0.25, 0.30 and 0.35 at different compositions described by the mole fraction x . This time the packing fraction is given by

$$\eta = \frac{\pi}{6} \rho \sum_i x_i d_i^3, \quad (9)$$

where

$$\rho = \sum_i \rho_i \quad (10)$$

is the total number density. At constant packing fraction, the total number density is changing.

The IGCMC results were compared with those calculated from the equation of Ebeling and Scherwinski [14]. The activity coefficients of the larger hard spheres are shown in Figure 2(a) and in Table 2. The simulations broke down for $x_2 = 0.1$ at $\eta = 0.30$ and for $x_2 = 0.1, 0.2$ and 0.3 at $\eta = 0.35$, because of the problem of inserting the larger molecules into the mixture with predominantly smaller molecules, arising from the lack of sufficient free space in a system. This problem does not occur in the calculation of activity coefficient for smaller molecules (Figure 2(b) and Table 3). As previously seen, the activity coefficient increases with increasing density of the system (Figure 2). Here, we further note that the activity coefficient of a mixture depends also on the mixture composition. The activity coefficient of larger molecules decreases (Figure 2(a)), while that of the smaller increases (Figure 2(b)) with increasing mole fraction of the component considered. We see that, at low concentration of larger molecules, their activity coefficient is greater than that of the pure component ($x_2 = 1$; Figure 2(a)). On the other hand, the activity coefficient of smaller spheres is lower than that

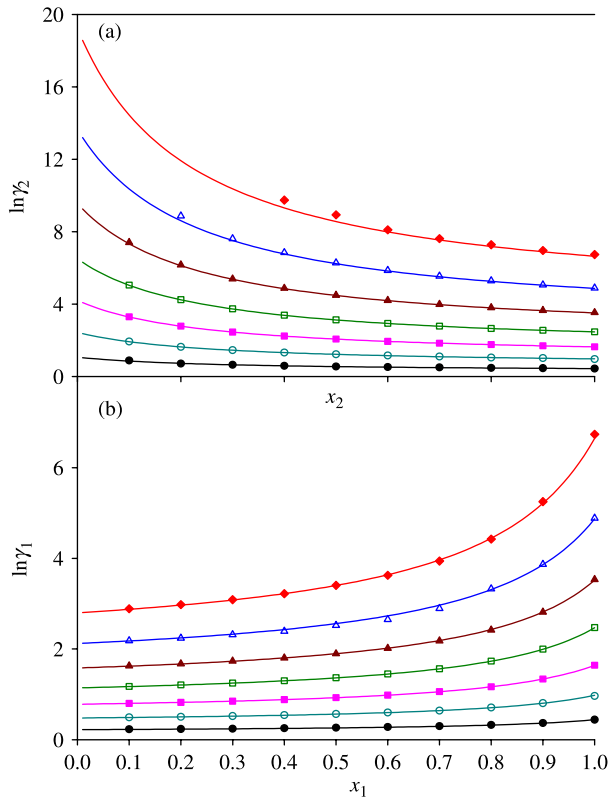


Figure 2 (Colour online). The individual activity coefficient of a binary hard-sphere mixture from IGCMC method (graphic characters) and from the Ebeling and Scherwinski equation (solid lines) for different x_2 (the snapshot a) and x_1 (the snapshot b) at the following η : 0.05, solid circles; 0.10, open circles; 0.15, solid squares; 0.20, open squares; 0.25, solid triangles; 0.30, open triangles; 0.35, solid diamonds.

of the pure component ($x_1 = 1$). This means that at a constant η the probability of insertion of a smaller sphere into a fluid of larger spheres is higher than the probability of insertion of a larger sphere into a fluid of smaller spheres.

4.3 SPM model

The next system studied was the SPM electrolyte model. Its thermodynamic properties, except for the individual activity coefficients, were intensively explored [15] by the MC simulations. We considered a 1:1 electrolyte at the total packing fraction of the solution $\eta = 0.3$ and at different electrolyte concentrations. To keep constant the packing fraction with the variation of the electrolyte concentration, the solvent concentration was changed. The temperature was 298.15 K and the relative permittivity $\epsilon_r = 78.5$. We considered systems with ions, d_{\pm} , and the solvent molecules, d_s of the same and different diameters. The first simulations were carried out for the same diameters of the ions and the solvent molecules. The results for $d = d_{\pm} = d_s = 300, 400$ and 500 pm are shown in Figure 3 by graphic characters and collected in Table 4. Additionally, Figure 3 presents the activity coefficients from the symmetric Poisson–Boltzmann (SPB) theory [11] (solid lines) and the mean-spherical approximation (MSA) [14] (dashed lines). The SPB activity coefficients were derived via the charging route for the individual ion activities, while the MSA equation was derived starting from a uniform neutralising background developed by Parrinello and Tosi [16]. In SPB and MSA, the solvent activity coefficients were calculated from the equation of Ebeling and Scherwinski [14]. It is interesting to note that the activity coefficient of the solvent, $\ln \gamma_s$, does not depend essentially on either the electrolyte concentration or the diameter d . The mean activity coefficient, $\ln \gamma_{\pm}$, of ions in the limit of zero electrolyte concentration has the same value as for the solvent molecules and decreases with increasing electrolyte concentration. The effect depends on the diameter, d . Although the SPB and MSA results diverge slightly from the IGCMC, their qualitative behaviour is similar. A better agreement with the MC results gives the SPB theory at low electrolyte concentration, while the MSA at higher concentrations. The divergence of the SPB results at high electrolyte concentration is perhaps due to the neglect of the

Table 2. Activity coefficients of larger hard spheres ($d_2 = 500$ pm) in a mixture with smaller ones ($d_1 = 300$ pm) (the IGCMC results).

x_2	$\ln \gamma$						
	$\eta = 0.05$	$\eta = 0.10$	$\eta = 0.15$	$\eta = 0.20$	$\eta = 0.25$	$\eta = 0.30$	$\eta = 0.35$
0.1	0.8806	1.9286	3.3003	5.0560	7.4012	–	–
0.2	0.7129	1.6385	2.7853	4.2500	6.1683	8.8690	–
0.3	0.6441	1.4520	2.4593	3.7430	5.3895	7.6170	–
0.4	0.5927	1.3240	2.2356	3.3913	4.8747	6.8490	9.7430
0.5	0.5520	1.2271	2.0706	3.1371	4.4910	6.2830	8.9360
0.6	0.5217	1.1550	1.9442	2.9376	4.2110	5.8620	8.1040
0.7	0.4975	1.0973	1.8448	2.7846	3.9870	5.5440	7.6210
0.8	0.4718	1.0496	1.7661	2.6605	3.8060	5.2960	7.2809
0.9	0.4578	1.0116	1.6981	2.5584	3.6540	5.0645	6.9642
1.0	0.4391	0.9629	1.6431	2.4734	3.5329	4.8898	6.7373

Table 3. Activity coefficients of smaller hard spheres ($d_1 = 300$ pm) in a mixture with larger spheres ($d_2 = 500$ pm) (the IGCMC results).

x_1	$\ln \gamma$						
	$\eta = 0.05$	$\eta = 0.10$	$\eta = 0.15$	$\eta = 0.20$	$\eta = 0.25$	$\eta = 0.30$	$\eta = 0.35$
0.1	0.2285	0.4902	0.8003	1.1734	1.6257	2.1835	2.8880
0.2	0.2339	0.5032	0.8238	1.2079	1.6751	2.2409	2.9810
0.3	0.2417	0.5198	0.8514	1.2496	1.7330	2.3151	3.0890
0.4	0.2502	0.5392	0.8844	1.3002	1.8031	2.3912	3.2210
0.5	0.2615	0.5643	0.9273	1.3659	1.8959	2.5214	3.4050
0.6	0.2767	0.5971	0.9832	1.4507	2.0138	2.6517	3.6260
0.7	0.2960	0.6409	1.0593	1.5660	2.1800	2.8932	3.9420
0.8	0.3228	0.7055	1.1680	1.7337	2.4197	3.3280	4.4250
0.9	0.3672	0.8040	1.3380	1.9976	2.8162	3.8690	5.2520
1.0	0.4391	0.9629	1.6431	2.4734	3.5329	4.8896	6.7374

fluctuation potential in the SPB theory and the choice of thermodynamic route [11].

It is worth noting that the behaviour of $\ln \gamma_{\pm}$ is different to that observed for the PM electrolyte [11]. In Figure 3, we do not observe a rise in $\ln \gamma_{\pm}$ at higher electrolyte concentrations characteristic of the PM electrolyte [6,8,11]. In PM, this increase is due to increased hard-sphere interactions at higher concentrations. In our case, the hard-sphere interactions are constant as the value of the packing fraction, η , is fixed and the diameters of all the components are the same. These interactions do not influence the characteristics of the ion activity coefficient curves, but only their values. The course depends on the inter-ionic electrostatic interactions including the exclusion volume and correlation effects. It is relevant to mention here that experiments have shown some electrolytes (e.g. aqueous KCl, KI, NaCl) to exhibit a concentration dependence of the mean activity coefficient similar to that shown in Figure 3 [17].

Next, we investigated a system with the ions and solvent molecules of different size (the diameters of the

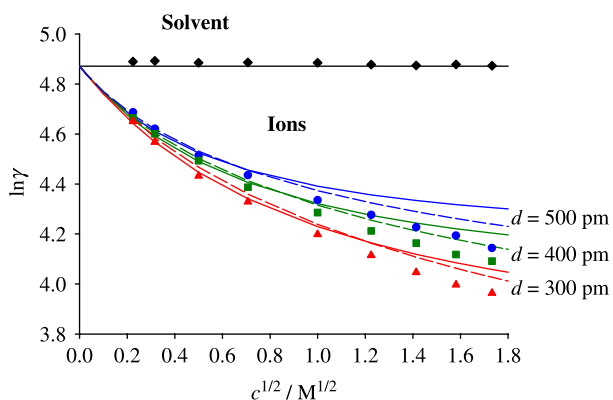


Figure 3 (Colour online). Dependence of the activity coefficient of ions and solvent for the SPM electrolyte at $\eta = 0.3$ on the electrolyte concentration for $d = 300, 400$ and 500 pm (graphic characters, IGCMC; solid lines, SPB; dashed lines, MSA).

anion and the cation being equal). First, the ion diameter was fixed at $d_{\pm} = 400$ pm, while the diameter of the solvent molecules d_s was 300, 400 or 500 pm. The other physical parameters were the same as for the earlier case of the common diameter. The ionic concentration dependence of the activity coefficients of ions and solvent molecules is given in Table 5 and illustrated in Figure 4(a),(b) by graphic characters. The corresponding SPB and MSA results are shown by the solid and dashed lines, respectively. Better agreement between the MC and the theoretical results is observed for the solvent. The mean activity coefficient of ions (Figure 4(a)) shows generally a decreasing tendency with increasing electrolyte concentration, however for $d_s = 500$ pm some increase is observed at high electrolyte concentrations. Even for the constant ion diameter, the mean activity coefficient depends on the solvent diameter. In a mixture with smaller solvent molecules, the mean activity coefficient is greater than in a mixture with larger molecules. The dependence of the activity coefficient of solvent (Figure 4(b)) on the electrolyte concentration varies: the curve for $d_s = 500$ pm is increasing, for $d_s = 300$ pm it is decreasing, while for

Table 4. The activity coefficient of ions and solvent for the SPM model at $\eta = 0.3$ (the IGCMC results).

c (M)	$d_{\pm} = d_s = 300$ pm		$d_{\pm} = d_s = 400$ pm		$d_{\pm} = d_s = 500$ pm	
	$\ln \gamma_{\pm}$	$\ln \gamma_s$	$\ln \gamma_{\pm}$	$\ln \gamma_s$	$\ln \gamma_{\pm}$	$\ln \gamma_s$
0.05	4.6507	4.8895	4.6645	4.8894	4.6868	4.8873
0.10	4.5681	4.8925	4.6010	4.8851	4.6214	4.8873
0.25	4.4323	4.8848	4.4935	4.8838	4.5135	4.8862
0.50	4.3288	4.8862	4.3875	4.8820	4.4354	4.8844
1.00	4.1982	4.8849	4.2861	4.8801	4.3353	4.8771
1.50	4.1147	4.8776	4.2123	4.8785	4.2765	4.8711
2.00	4.0466	4.8743	4.1634	4.8743	4.2269	4.8600
2.50	3.9965	4.8785	4.1179	4.8717	4.1934	4.8584
3.00	3.9637	4.8730	4.0912	4.8637	4.1437	4.8336

Table 5. The activity coefficients of ions and solvent for the SPM model at $\eta = 0.3$, $d_{\pm} = 400$ pm for different solvent diameters (the IGCMC results).

c (M)	$d_s = 300$ pm		$d_s = 400$ pm		$d_s = 500$ pm	
	$\ln \gamma_{\pm}$	$\ln \gamma_s$	$\ln \gamma_{\pm}$	$\ln \gamma_s$	$\ln \gamma_{\pm}$	$\ln \gamma_s$
0.05	8.3259	4.8743	4.6645	4.8894	3.1037	4.9042
0.10	8.1975	4.8568	4.6010	4.8851	3.0417	4.9203
0.25	7.9975	4.8142	4.4935	4.8838	2.9671	4.9645
0.50	7.7784	4.7490	4.3875	4.8820	2.9182	5.0505
1.00	7.4055	4.6113	4.2861	4.8801	2.9021	5.1957
1.50	7.0683	4.4748	4.2123	4.8785	2.9461	5.3715
2.00	6.7451	4.3404	4.1634	4.8743	2.9932	5.5276
2.50	6.4551	4.2080	4.1179	4.8717	3.0497	5.6831
3.00	6.1844	4.0725	4.0912	4.8637	3.1116	5.8348

$d_s = 400$ pm it is constant and this is the case discussed earlier.

The next simulations were performed for the fixed diameter of the solvent molecules, $d_s = 400$ pm and for the following ion diameters: $d_{\pm} = 300, 400$ and 500 pm. The IGCMC results are shown in Figure 5 by graphic characters and collected in Table 6. The solid and dashed

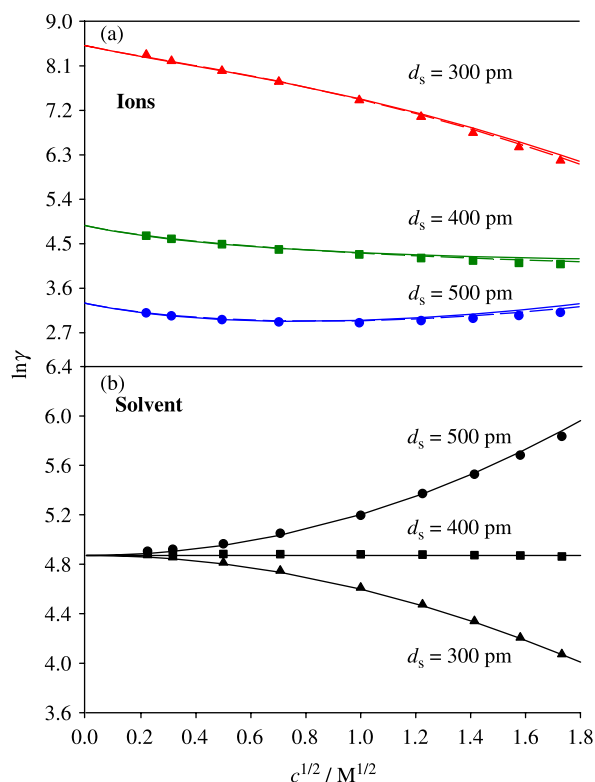


Figure 4 (Colour online). Dependence of the activity coefficient of ions (a) and solvent (b) for the SPM electrolyte at $\eta = 0.3$ on the electrolyte concentration for $d_{\pm} = 400$ pm and $d_s = 300, 400$ and 500 pm (graphic characters, IGCMC; solid lines, SPB; dashed lines, MSA).

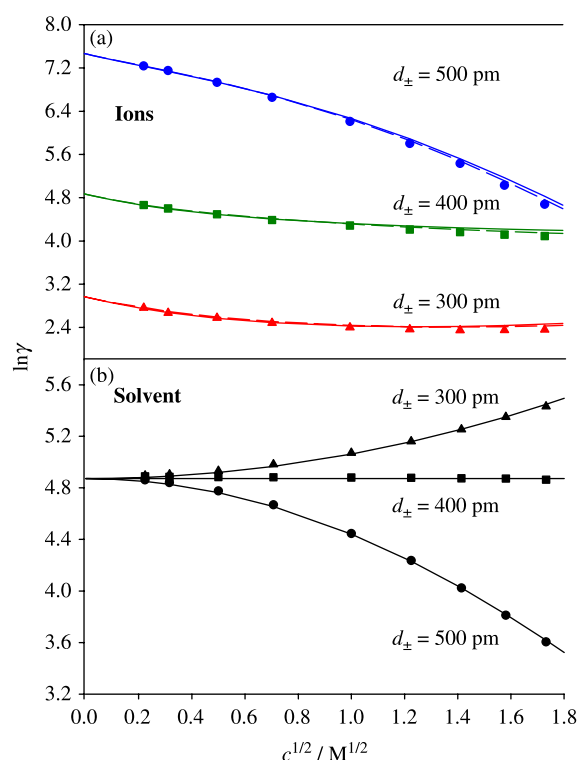


Figure 5 (Colour online). Dependence of the activity coefficient of ions (a) and solvent (b) for the SPM electrolyte at $\eta = 0.3$ on the electrolyte concentration for $d_s = 400$ pm and $d_{\pm} = 300, 400$ and 500 pm (graphic characters, IGCMC; solid lines, SPB; dashed lines, MSA).

lines in Figure 5 show the SPB and MSA results, respectively. The mean activity coefficient decreases with increasing electrolyte concentration (Figure 5(a)), although a slight rise at higher concentrations is observed. Its value evidently depends on the ion diameters: the larger the ions, the greater the activity coefficient. The dependence of the activity coefficient of solvent on

Table 6. The activity coefficient of ions and solvent for the SPM model at $\eta = 0.3$, $d_s = 400$ pm for different ion diameters (the IGCMC results).

c (M)	$d_{\pm} = 300$ pm		$d_{\pm} = 400$ pm		$d_{\pm} = 500$ pm	
	$\ln \gamma_{\pm}$	$\ln \gamma_s$	$\ln \gamma_{\pm}$	$\ln \gamma_s$	$\ln \gamma_{\pm}$	$\ln \gamma_s$
0.05	2.7623	4.8959	4.6645	4.8894	7.2361	4.8611
0.10	2.6706	4.9037	4.6010	4.8851	7.1516	4.8403
0.25	2.5770	4.9323	4.4935	4.8838	6.9340	4.7753
0.50	2.4832	4.9827	4.3875	4.8820	6.6554	4.6675
1.00	2.3993	5.0710	4.2861	4.8801	6.2097	4.4457
1.50	2.3658	5.1603	4.2123	4.8785	5.8025	4.2359
2.00	2.3478	5.2532	4.1634	4.8743	5.4336	4.0232
2.50	2.3519	5.3502	4.1179	4.8717	5.0290	3.8118
3.00	2.3614	5.4316	4.0912	4.8637	4.6783	3.6052

the electrolyte concentration (Figure 5(b)) varies again, but this time the curve for $d_{\pm} = 300$ pm increases while for $d_{\pm} = 500$ pm it decreases. The curve for $d_{\pm} = 400$ pm is flat.

It can be clearly seen from Figures 2, 4 and 5 that the smaller molecules in a mixture with larger ones have a lower activity coefficient than the larger molecules in a mixture with smaller ones at the same packing fraction of a system. This effect can be explained by the fact that the probability of insertion of smaller molecules into the system with a predominance of larger molecules is higher than that of the reverse situation.

5. Conclusions

The principal achievement of this paper has been a successful implementation of the IGCMC technique in calculating the activity coefficient of a high density fluid. Our calculations for the binary mixtures clearly indicate that smaller molecules have lower activity coefficient than the larger ones. This finding allows an explanation of the unexpected adsorption behaviour of Cs^+ cations from the mixed electrolyte with Li^+ or Mg^{2+} ions at the negatively charged Langmuir film noticed by Shapovalov and Brezesinski [18]. They found that the adsorption of Cs^+ cations of the smallest hydrated radius, in comparison with the adsorption of larger Li^+ and divalent Mg^{2+} , is stronger than one could expect. Earlier, this behaviour was confirmed by the volume corrected Poisson–Boltzmann equation [19] and by the MC simulations [20]. Also the present results indicate that adsorption of smaller ions, which have the lower activity coefficient and thus the lower chemical potential, should be enhanced. Finally, we would like to notice that although we intended to use the SPB and MSA theories to test the IGCMC method, we have shown that these theories could be applied successfully to the SPM electrolyte with the realistic concentrations of ions and solvent molecules.

Acknowledgements

The authors are very grateful to Professors C.W. Outhwaite and L.B. Bhuiyan for their comments and suggestions and for making available their SPB program. Financial support from Adam Mickiewicz University, Faculty of Chemistry, is appreciated.

References

- [1] M.P. Allen and D.J. Tildesley, *Computer Simulation of Liquids*, Clarendon Press, Oxford, 1987, pp. 49–50.
- [2] B. Widom, *Some topics in the theory of fluids*, J. Chem. Phys. 39 (1963), pp. 2808–2812.
- [3] P. Sloth and T.S. Sørensen, *Monte Carlo simulations of single-ion chemical potentials. Preliminary results for the restricted primitive model*, Chem. Phys. Lett. 143 (1988), pp. 140–144.
- [4] P. Sloth and T.S. Sørensen, *Monte Carlo simulations of single ion chemical potentials. Results for the unrestricted primitive model*, Chem. Phys. Lett. 146 (1988), pp. 452–455.
- [5] D.J. Adams, *Chemical potential of hard-sphere fluids by Monte Carlo methods*, Mol. Phys. 28 (1974), pp. 1241–1252.
- [6] J.P. Valleau and L.K. Cohen, *Primitive model electrolytes. I. Grand canonical Monte Carlo computations*, J. Chem. Phys. 72 (1980), pp. 5935–5941.
- [7] J.P. Valleau, L.K. Cohen, and D.N. Card, *Primitive model electrolytes. II. The symmetrical electrolyte*, J. Chem. Phys. 72 (1980), pp. 5942–5954.
- [8] S. Lamperski, *The individual and mean activity coefficients of an electrolyte from the inverse GCMC simulation*, Mol. Simul. 33 (2007), pp. 1193–1198.
- [9] A. Malasics, D. Gillespie, and D. Boda, *Simulating prescribed particle densities in the grand canonical ensemble using iterative algorithms*, J. Chem. Phys. 128 (2008), 124102.
- [10] P. Sloth and T.S. Sørensen, *Single-ion activity coefficients and structure of ionic fluids. Results for the primitive model of electrolyte solutions*, J. Phys. Chem. 94 (1990), pp. 2116–2223.
- [11] M. Molero, C.W. Outhwaite, and L.B. Bhuiyan, *Individual ionic activity coefficients from a symmetric Poisson–Boltzmann theory*, J. Chem. Soc., Faraday Trans. 88 (1992), pp. 1541–1547.
- [12] C.W. Outhwaite, M. Molero, and L.B. Bhuiyan, *Primitive model electrolytes in the modified Poisson–Boltzmann theory*, J. Chem. Soc., Faraday Trans. 89 (1993), pp. 1315–1320.
- [13] C.W. Outhwaite, M. Molero, and L.B. Bhuiyan, *Corrigendum to primitive model electrolytes in the modified Poisson–Boltzmann theory*, J. Chem. Soc., Faraday Trans. 90 (1994) p. 2002.
- [14] W. Ebeling and K. Scherwinski, *On the estimation of theoretical individual activity coefficients of electrolytes*, Z. Phys. Chem. (Leipzig) 264 (1983), pp. 1–14.
- [15] J. Reščič, V. Vlasy, L.B. Bhuiyan, and C.W. Outhwaite, *Monte Carlo simulations of a mixture of an asymmetric electrolyte and a neutral species*, J. Chem. Phys. 107 (1997), pp. 3611–3618.
- [16] M. Parrinello and M.P. Tosi, *Analytic solution of the mean spherical approximation for a multi-component plasma*, Chem. Phys. Lett. 64 (1979), pp. 579–581.
- [17] D.R. Lide, *Handbook of Chemistry and Physics*, 88th Edition 2007–2008, Taylor & Francis Group Press, LLC (2008), pp. 5-79 – 5-84.
- [18] V.L. Shapovalov and G. Brezesinski, *Breakdown of the Gouy–Chapman model for highly charged Langmuir monolayers: Counterion size effect*, J. Phys. Chem. B 110 (2006), pp. 10032–10040.
- [19] P.M. Biesheuvel and M. Soestbergen, *Counterion volume effects in mixed electrical double layers*, J. Colloid Interface Sci. 316 (2007), pp. 490–499.
- [20] S. Lamperski and C.W. Outhwaite, *Monte-Carlo simulation of mixed electrolytes next to a plane charged surface*, J. Colloid Interface Sci. 328 (2008), pp. 458–462.